Uncertainty analysis for the nuclear liquid drop model and implications for the symmetry energy coefficients

Yuping Cao and Danhui Lu◉

Department of Applied Physics, Nanjing University of Science and Technology, Nanjing 210094, China

Yibin Qian*

Department of Applied Physics, Nanjing University of Science and Technology, Nanjing 210094, China
and MIIT Key Laboratory of Semiconductor Microstructure and Quantum Sensing,
Nanjing University of Science and Technology, Nanjing 210094, China

Zhongzhou Ren

School of Physics Science and Engineering, Tongji University, Shanghai 200092, China

Background: Despite its age, the nuclear liquid drop (LD) model, plus the microscopic corrections, still plays an important role in nuclear mass studies. Especially, the LD model readily correlate the finite nucleus and the nuclear matter through the symmetry energy term.

Purpose: To systematically analyze the model uncertainty of the LD mass formula and check the corresponding symmetry energy coefficients.

Method: The Monte Carlo bootstrap approach, based on the nonparametric sampling, is applied to determine the statistical uncertainties of the parameter set in two popular LD formulas. The dependence between these parameters is also quantified via the correlation coefficients.

Results: The least required proportion of the experimental mass data is fixed for the fitting process of the LD formula. After the statistical deviation is determined for each parameter in the LD formula, the model uncertainty is evaluated as illustrated for one heavy isotopic chain. The Pearson coefficients between each two parameters involved in the LD mass formula are tabulated and figured plus the detailed discussions on the surface and volume symmetry energy coefficients.

Conclusion: The uncertainties of the fitted parameters and the LD model itself are smooth, leading to a relatively stable extrapolation. It is necessary to include the Wigner energy term in the LD model when yielding the reasonable symmetry energy coefficients.

I. INTRODUCTION

Mass is a fundamental entity of all matter. In atomic nuclei, mass appears in the form of the binding energy of the nuclear constituents. This is of particular physical importance as it strongly depends on the nuclear force for which a general expression is still unknown [1]. The nuclear mass is also crucial for unraveling the rapid neutron-capture process or the *r*-process regulating the formation and evolution of heavy elements in universe [2]. However, the present experimental facilities aimed at the nuclear mass are still not accessible to these short-lived nuclei in the *r*-process path [3]. As a result, the theoretical mass evaluations are urgently required especially towards the high-precision extrapolation. Up to now, the well-known global mass models are generally constructed based on the macroscopic- (mac-) microscopic (mic) approach (such as the finite range droplet

model [4,5] and the Weizsäcker-Skyrme formula [6,7]), Hartree-Fock-Bogoliubov method [8,9], the Dulflo-Zuker (DZ) shell-model scheme [10], and the nuclear density-functional theory [11,12]. On the other hand, the local tool, rooted in the Garvey-Kelson relationship [13,14], the *n*-*p* residual interaction [15] and so on, is exploited to evaluate and predict the nuclear binding energy in an effective way. Among these current mass formulas, the traditional nuclear liquid drop (LD) model deserves special attention due to its tremendous success in understanding the systematics of the binding energy per nucleon and the nuclear fission process at the early stage of nuclear physics. The consensus is that the simple LD formula is inspired from two essential properties of the atomic nucleus, namely, its incompressibility and the saturation of nuclear force between nucleons. Meanwhile, the liquid drop part governs the general trend of the nuclear binding energy variation in the aforementioned mac-mic and DZ models. When the mass number in the LD formula approaches the infinity, the residual part is the symmetry energy, which is supposed to be connected with the same term in the

---

*qyibin@njust.edu.cn

equation of state (EOS) of nuclear matter. This has been curved as a generic relation between the symmetry energy coefficient of finite nuclei and that of nuclear matter [16]. After the introduction of more structural ingredients, the LD formula has been further improved to obtain more accurate binding energy values [17] or the mass difference (such as α-decay energies) [18] as well.

When the uncertainty analysis was placed on the nuclear mass fits, the liquid drop formula was taken as a pioneering laboratory to study the model errors within the regression method plus the possible extension to microscopic corrections [19–21]. Recently, the machine learning strategy has been introduced into the modern mass formulas, to improve their accuracies and predictive abilities especially towards the unmeasured region of nuclear chart [11,22–27]. In the meantime, the model uncertainty can be estimated simultaneously during these procedures, such as the Bayesian inference plus the Monte Carlo Markov chain-sampling [11,24–26]. Besides, the nonparametric resampling method can be another choice in the statistics practice [28–30], which has been implemented in nuclear physics via the bootstrap procedure [31–33]. It is, therefore, interesting to apply the Monte Carlo bootstrap method into the uncertainty analysis of nuclear mass evaluations. As is well known, the overfitting problem may exist due to the complexity of model mass formulas, which can hamper the reliability of theoretical extrapolations. To somewhat avoid this issue for nuclear mass, the (least) required amount of involved samples in the LD fitting will be carefully explored to be helpful in the parameter determining of other mass models. Through the repetitive and random sampling, the bootstrap can help us to discuss the correlation between model parameters, which is beneficial to understand the physics of each term when there are usually many parameters in both semimic and microscopic mass formulas. A noteworthy point is that one can then obtain the huge groups of volume and surface symmetry energy coefficients (SEC) plus their ratios in the LD formula, leading to a error analysis on the SEC of equation of state in nuclear matter derived from the above-mentioned relationship about the symmetry energy [16]. In the next section, two selected LD formulas are given following by the brief introduction of the bootstrap method. The detailed results on the model uncertainty and other quantities are then presented and discussed in Sec. III, and a short summary is given in Sec. IV.

II. LIQUID DROP MODEL AND STATISTICAL METHOD

There are two types of liquid drop models used here, namely, a slightly modified version of Bethe and Weizsäcker (BW) formula [34] and an extended expression taken from Ref. [17]. The former BW binding energy is composed of volume, surface, Coulomb, symmetry, and pairing terms, given as [35,36]

$$B = a_v A + a_s A^{2/3} + a_C \frac{Z^2}{A^{1/3}} + a_{\mathrm{sym}} \frac{(N-Z)^2}{A} + a_{\mathrm{ssym}} \frac{(N-Z)^2}{A^{4/3}} + a_p \frac{\delta(N,Z)}{\sqrt{A}}, \quad (1)$$

where $\delta(N, Z) = [(-1)^Z + (-1)^N]/2$, and the surface term (a_{ssym}) make the symmetry energy adjusted to the finite nuclei so that the $(a_{\mathrm{sym}} + a_{\mathrm{ssym}}/A^{1/3})$ is usually called the symmetry energy coefficient $a_{\mathrm{sym}}(A)$ of finite nuclei. The latter one is sensitively related to the symmetry energy of asymmetric nuclear matter, which will be paid special attention in this study. After introducing some extra ingredients, the BW mass formula can be modified as

$$B = a_v A + a_s A^{2/3} + a_C \frac{Z^2}{A^{1/3}} + a_{\mathrm{sym}} \frac{(N-Z)^2}{A} + a_{\mathrm{xC}} \frac{Z^{4/3}}{A^{1/3}}$$
$$+ a_W \frac{|N-Z|}{A} + a_{\mathrm{ssym}} \frac{(N-Z)^2}{A^{4/3}} + a_p \frac{\delta(N,Z)}{\sqrt{A}}$$
$$+ a_R A^{1/3} + a_{\mathrm{sh1}} P + a_{\mathrm{sh2}} P^2, \quad (2)$$

where the subscripts xC, W, R, sh1, and sh2 denote the exchange Coulomb, Wigner, curvature terms, and empirical shell corrections, respectively. The Casten factor P is defined as [37]

$$P = \frac{v_n v_p}{v_n + v_p}, \quad (3)$$

where v_n and v_p mean the number of valence nucleons derived from the subtraction between the proton (neutron) numbers and the nearest magic numbers. For convenience, Eqs. (1) and (2) are separately denotes as "LD1" and "LD2" in the following. On the basis of the two above LD formulas, the uncertainty analysis is implemented through the bootstrap statistical method as follows [31–33]:

(1) The experimental binding energy data from the atomic mass evaluation table [38] with the error bar below 100 keV are selected as the learning set, namely, $\{B_k\}$ with the total number of $N = 2184$. The subscript k symbolizes one specific nucleus in this total set. These measured data are considered as the accurate values due to their high precision. In the traditional bootstrap procedure, N samples are picked up from the learning set $\{B_k\}$ with the permission of the replacement (one key factor in this kind of statistic analysis). Differently, the present number of picked samples is M, smaller than N, i.e., $M < N$. For each sampling with M, one will get the standard deviation $\hat{\sigma}$ between evaluated binding energies and the experimental data after the fitting process. The $\hat{\sigma}$ value can be plotted versus M or the ratio r of M to the total number N.

(2) The above plotting or analysis is to be repeated more than 1000 times to fix the M or r value, above which the standard deviation would be steady and stable. Within this fixed sampling ratio, the bootstrap strategy is then employed for two LD mass formulas. For the ith sampling, one can obtain an binding energy array $\{B_{k'}^i\}$, and the parameter set of LD formula is determined by matching these chosen experimental values. The subscript k' is same as the above k but for the fixed M samples. This process will be repeated again and again to get $T = 10^4$ groups of parameters for each LD mass formula.

(3) With these obtained parameters sets, the uncertainty evaluation plus the correlation analysis between different terms can be proceeded. For these nuclei with measured mass data, the systematical error is estimated as

$$\hat{\sigma}^2_{\text{sys},k} = (\bar{B}_{k,\text{cal}} - B_{k,\text{exp}})^2, \tag{4}$$

where $\bar{B}_{k,\text{cal}}$ is the mean value of the calculated results for the kth nucleus, i.e., $\bar{B}_{k,\text{cal}} = \frac{1}{T}\sum_{i=1}^{T} B^i_{k,\text{cal}}$. In the meantime, the statistical uncertainty is assessed by the unbiased square deviation of the computed binding energies themselves,

$$\hat{\sigma}^2_{\text{stat},k} = \frac{1}{T-1}\sum_{i=1}^{T} \left(B^i_{k,\text{cal}} - \bar{B}_{k,\text{cal}}\right)^2. \tag{5}$$

When extrapolating to the unknown mass region, this statistical error can be used to evaluate the model uncertainty itself. In addition, one can also figure out the uncertainty of the coefficient $a_{\text{sym}}(A)$ in the LD mass formula of finite nuclei from the obtained T groups of parameters. This is instrumental for governing the symmetry energy in the equation of state of asymmetric nuclear matter [16,39].

III. NUMERICAL RESULTS AND DETAILED DISCUSSIONS

As above mentioned, the special attention is paid to an interesting question: How many learning samples do we, at least, need to derive a mass formula so that the latter can be able to reasonably produce the binding energies of all known nuclei? Although this procedure is performed here only for the LD model, the conclusion could be valuable for other mass formulas, and it can be easily reperformed there. Meanwhile, this kind of discussion on the required fitting data is expected to be meaningful for not only somewhat overcome the overfitting problem, but also reducing the massive computation cost when it comes to the complicated- (mac-) microscopic calculations. For each sampling, one picks up M binding energies of nuclei from the total learning set and then determines the parameters of the LD formula by fitting these selected samples. With this parameter set, we calculate the standard deviation among calculated binding energies, experimental values for the selected samples, the total measured nuclei, and the residual ones. All these three kinds of $\hat{\sigma}$ are plotted versus the ratio of the selected M nuclei to the total data for many times (over 1000 times), two of which are arbitrarily chosen and presented in Fig. 1 for the cases LD1 and LD2, respectively.

From Fig. 1, one can easily get one point that the deviation value of the total learning nuclei generally hold as a constant beyond one specific ratio (about 30%). This implies that this ratio of fitting samples is big enough for regulating the mass formulas or, at least, the LD ones. On the other hand, the $\hat{\sigma}$ values of selected and residual samples vary around the total deviation as accompanied by the random pattern. This can be easily understood from the fact that there are different microscopic influences, such as the shell and pairing corrections,
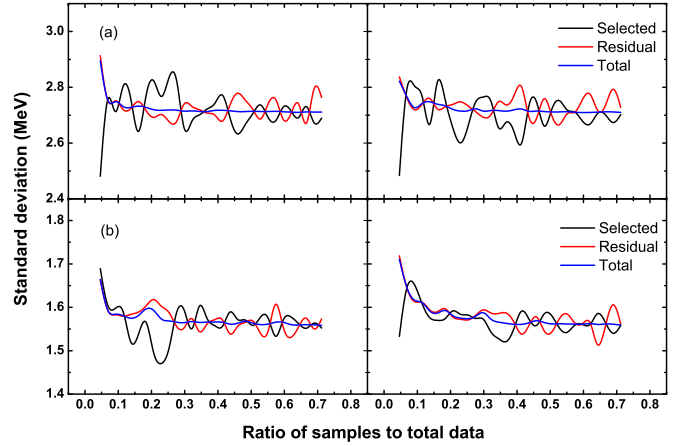

FIG. 1. Standard deviation between the calculated binding energies and the experimental values versus the sampling ratio with respect to the total experimental data, for (a) LD1 and (b) LD2, respectively. Note that the black, red, and blue lines are, respectively, for the selected samples, residual nuclei, and total measured nuclei.

beyond the LD benchmark in different regions of nuclear chart. Given the random sampling, the occurrence of the structural influence is also arbitrary, resulting in the oscillation of the corresponding $\hat{\sigma}$ value. However, these special deviations away from the LD baseline, such as the closed-shell nuclei, are covered in the mean-value process for the total nuclei. Hence, with the increasing of the ratio of the samples, the $\hat{\sigma}$ line of selected samples approaches that of total nuclei. On the other hand, the situation of the residual nuclei is kind of in the opposite direction in view of the fixed total nuclei, leading to the reverse phase pattern there as compared to the selected samples. Of course, note that the amplitude of these oscillations of the black and red lines in Fig. 1 is limited in contrast with the total $\hat{\sigma}$ value, implying the robustness of the LD-type formula. In general, the total deviation changes very smoothly despite the relatively large value itself, indicating that the basic features of nuclear masses have been grasped in the LD framework.

As mentioned in the above section, the bootstrap procedure is then implemented within the fixed sampling ratio, namely 30%. Once the T groups of parameters are obtained, one can, subsequently, get two important messages, i.e., the uncertainty of parameters and the correlation between them. This can be not only beneficial for understanding the physics behind the mass formulas plus the reduction of parameters, but also bring us the uncertainty evaluation of the model and its prediction. In addition, the parameter pattern of LD1 is supposed to be covered by the LD2 case, which is indeed the realistic situation when we proceeded the uncertainty analysis on the two types of LD formulas. Hence, the following results and discussions are mainly based on the LD2 formula for simplicity without hampering the following conclusion.

Table I presents the chosen range of involved coefficients in the LD2 mass formula in which the statistical deviation (uncertainty) of each parameter is calculated as $\sigma_i = \sqrt{\frac{1}{T-1}\sum_{j=1}^{T}(a_i^j - \bar{a}_i)^2}$, where the mean value of a_i equals to

TABLE I. Detailed results of the parameter set (scale in MeV) in the LD2 formula, including the mean value, the statistical deviation, the maximum, and the minimum values plus the relative uncertainty.

|	$\bar{a}_i$	σ_i	max	min	$|\sigma_i/\bar{a}_i|$ (%)
a_V	-16.5158	0.1108	-16.1034	-16.9181	0.67
a_S	26.2087	0.7107	28.7784	23.3157	2.71
a_C	0.7664	0.0046	0.7834	0.7478	0.60
a_{sym}	32.0407	0.5036	34.0229	30.1952	1.57
a_{xC}	-1.9588	0.1262	-1.5329	-2.4656	6.44
a_W	55.7071	5.3123	79.1552	35.2188	9.54
a_{ssym}	-59.3384	2.6639	-49.4875	-69.1303	4.49
a_p	-10.7484	0.7250	-8.2585	-13.8036	6.75
a_R	-14.1299	1.2957	-9.1116	-19.2447	9.17
a_{sh1}	1.8538	0.0852	2.1932	1.5254	4.60
a_{sh2}	-0.1356	0.0087	-0.1028	-0.1682	6.42

FIG. 2. Comparison of the calculated binding energies from LD2 with the available experimental ones for the uranium isotopes where the statistical error of each nucleus is separately demonstrated in large scale to guide the eye.

$\sum_{j=1}^{T} a_i^j$. The relative uncertainty $\sigma_i/\bar{a}_i$ is also listed in the last column to further show the varying scale of each coefficient. It is obvious that the volume and Coulomb terms are the most stable, whereas the Wigner and curvature parameters change relatively dramatically. Indeed, it is commonly accepted that the volume part of the binding energy should be proportional to the mass number A due to the short-range nature of nuclear force [17,34]. Meanwhile, the nucleus is addressed as a uniformly charged sphere plus the well-known electromagnetic interaction, resulting in the relatively clear Coulomb energy. In contrast, despite the recognition of Wigner term, its specific expression still appears to be diverse [6,40]. The physics resource is not explicit for the introduction of curvature term either. In addition, the surface and symmetry energies are believed to be indispensable whereas the choices of other terms are actually not definitive. For example, the empirical shell correction comes from the valence nucleon scheme, which is sensitively dependent on the shell position, whereas the evolution of shell closure is supposed to occur in neutron-rich nuclei.

Given the above uncertainties of the coefficients, the corresponding error bars, especially towards the border region of nuclear chart, should be quite valuable in the point of view of the model prediction. This statistical deviation somewhat determines to what extent can we trust the mass formula. The detailed results of the isotopic chain of uranium, the heaviest natural element (up to now), are presented in Fig. 2 to illustrate the former point. As additional information, other evaluations generally behave in a similar way. From this figure, one can see that the theoretical results are in reasonable agreement with the available experimental data. When it comes to the neutron-rich region, there is a clear convergent tendency for the binding energy, correlating to the saturation properties of nuclear force. For a better insight into the model uncertainty, this quantity is shown in the embedded figure. As can be seen, the statistical error will increase with the increasing of mass (neutron) number. Specifically, the uncertainty value is about 4.5 MeV in the vicinity of the predicted neutron dripline, which is compatible to the standard deviation of the LD itself as shown in Fig. 1. It may be concluded that
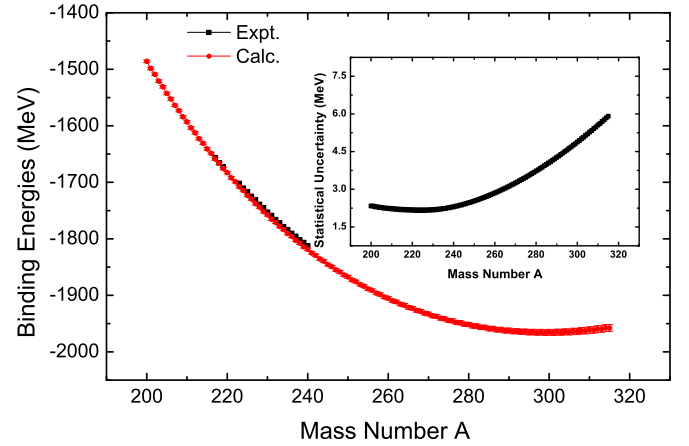
the liquid drop mass formula can, at least, offer a relatively robust extrapolating trend excluding the systematic error. As noted previously, another merit of the present nonparametric sampling is the direct correlation analysis of parameters involved in the theoretical model. Owing to the accumulation of T groups of parameters from the above resampling procedure, each coefficient is plotted versus all the other ones in Fig. 3 in which one can easily pick up the parameters with a strong linear relationship. In detail, this group of pictures are mapped into the matrix of the Pearson correlation coefficients between each two parameters from the LD2 formula as shown in Table II. As expected, the three dominant terms, namely, the volume, surface, and Coulomb energies, are correlated closely with each other [17,34]. Provided the volume and surface terms, the liquid drop mass formula can be assumed as an expansion in powers of $A^{-1/3}$, naturally generating the curvature part in terms of $a_R A^{1/3}$ [17]. These three terms are indeed related clearly with each other as indicated by their correlation coefficients. The shell correction is based on the valence correlation scheme up to the second order, resulting in the obvious correlation between them.

Last but not least, let us pay special attention to the symmetry energy and the Wigner energy for masses of finite nuclei. The symmetry energy is not only supposed to be crucial for compensating the discrepancies between different mass formulas towards the dripline of nuclear chart [36,41], but also play a key role in constraining the EOS in nuclear matter [16,35,39,42–44]. In this sense, it is of physical interest to see what will happen with regarding to the behavior of symmetry energy in nuclear mass after the proceeding of the present statistical analysis. The symmetry energy coefficient is here adopted as $a_{\mathrm{sym}} = (a_{\mathrm{sym}} + a_{\mathrm{ssym}}/A^{1/3})$ in which the two parameters are found to correlate greatly with the Wigner term coefficient as can be seen from both Fig. 3 and Table II. One can, therefore, conjecture that the introduction of the Wigner energy is necessary to correctly extract the symmetry energy coefficient from the nuclear mass data. According to the seniority shell model or the Wigner
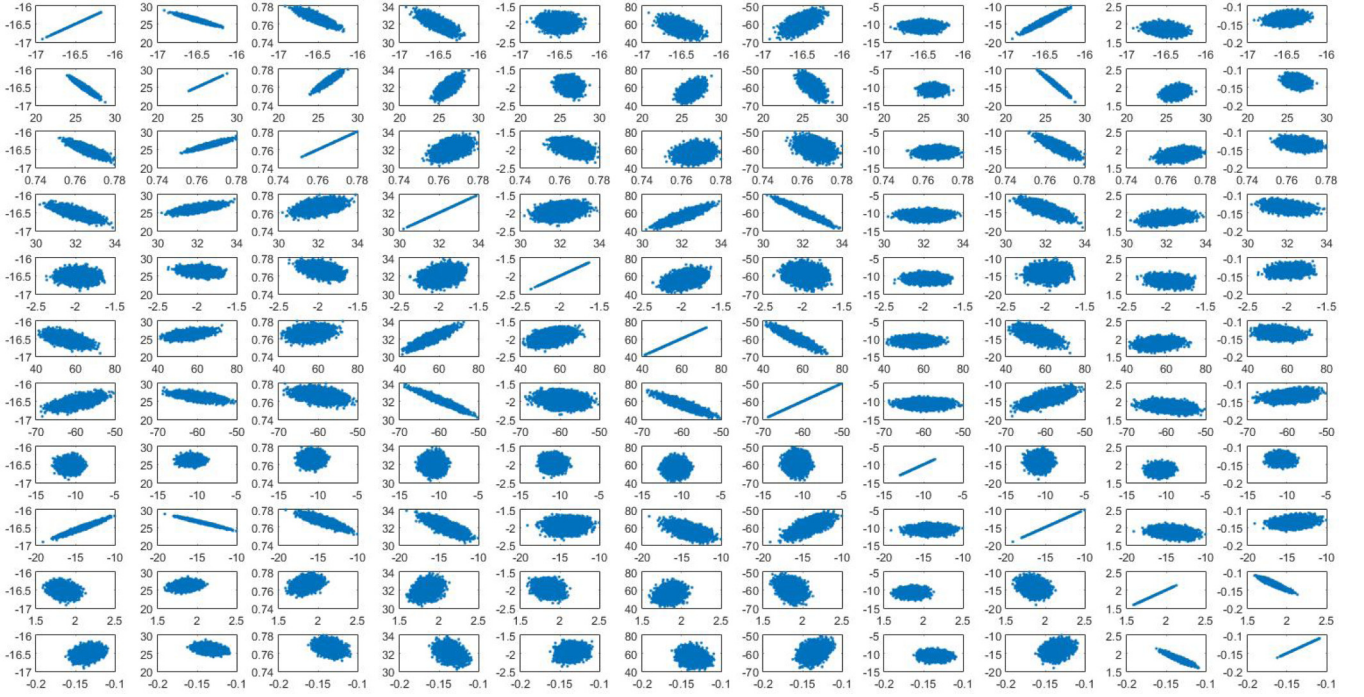
FIG. 3. Sketch of correlation between each other in all the obtained parameters of LD2 through the large-scale samplings. Note that the plotting is made on the order of occurrence of each term in Eq. (2).

supermultiplet theory [17,45], the isospin dependence of the nuclear ground-state energies would actually behave in the $T(T + 1)$ or $T(T + 4)$ form with $T = |N - Z|/2$. Hence, there should be a linear T-dependent term, referred as the Wigner term [46,47], besides the conventional symmetry energy $(N - Z)^2/A$. On the other hand, the coefficient of Wigner energy is in strong correlation with those of symmetry energy as shown in Table II. One can then speculate that the loss of the Wigner energy would be compensated in the symmetry energy coefficient during the fitting process. To put forward this, the two parameters a_{sym} and a_{ssym} are also extracted based on the LD1 formula (without the Wigner term) via the bootstrap method. Besides this, the same procedure is performed again after these nuclei around the shell closure

are cleared out to avoid the shell effect as much as possible. In detail, if the difference between the proton (neutron) number of a nucleus and the nearest magic number is less than four, this nucleus is excluded in the sampling procedure. Within the present SEC form $a_{sym}(A)$, the $a_{sym} = 26.55 \pm 0.23$ and $a_{ssym} = -18.87 \pm 1.23$ MeV is determined for the LD1 case via the aforementioned analysis on 10 000 times of samplings, whereas these two parameter vary quite limitedly with the exclusion of near-shell nuclei, namely, $a_{sym} = 26.65 \pm 0.23$ and $a_{ssym} = -19.12 \pm 1.27$ MeV. As expected, the shell effect on the extraction of symmetry energy coefficient appears to be limited, which is consistent with conclusion from the systematics of double β-decay energies in Ref. [48]. Meanwhile, the extracted value of a_{sym} is not consistent with the

TABLE II. Pearson correlation coefficients between each two parameters involved in the LD2 mass formula, corresponding to Fig. 3. Those correlation coefficients, above 0.9, are denoted as bold, implying the strong linear relationship between the corresponding energy terms. Only the half of this symmetric matrix is shown for simplicity without hampering the presentation.

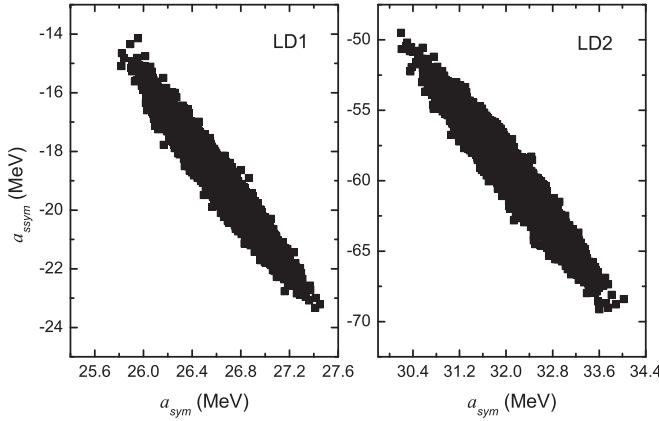|	a_V	a_S	a_C	a_{sym}	a_{xC}	a_W	a_{ssym}	a_p	a_R	a_{sh1}	a_{sh2}
a_V		**−0.949**	−0.842	−0.783	−0.041	−0.584	0.669	0.033	**0.968**	−0.214	0.202
a_S			**0.933**	0.679	−0.259	0.454	−0.619	−0.038	**−0.980**	0.228	−0.198
a_C				0.447	−0.472	0.195	−0.388	−0.036	−0.851	0.277	−0.226
a_{sym}					0.331	**0.903**	**−0.967**	−0.009	−0.775	0.262	−0.291
a_{xC}						0.482	−0.210	0.014	0.097	−0.128	0.061
a_W							**−0.912**	−0.014	−0.597	0.193	−0.203
a_{ssym}								0.009	0.713	−0.277	0.292
a_p									0.041	−0.043	0.047
a_R										0.229	0.208
a_{sh1}											**−0.951**
a_{sh2}											

FIG. 4. Correlation between the original symmetry energy coefficient a_{sym} and the surface correction one a_{ssym} for the LD1 and LD2 cases, respectively.

commonly reported one, such as 30–32 MeV [41]. In contrast, the optimal $a_{\text{sym}} = 32.04 \pm 0.50$ and $a_{\text{ssym}} = -59.34 \pm 2.66$ MeV is determined for the LD2 case, which seems to be more reasonable. Based on the above discussion and other careful comparisons [6,49], the Wigner energy is indeed responsible for such a kind of symmetry energy pattern. Note that the shell correction, as mentioned in Ref. [48], is important for the reasonable extraction of the coefficient of the Wigner energy due to the comparable magnitude between them. To get an insightful view, the original symmetry energy coefficient a_{sym} is plotted versus the surface correction term a_{ssym} in Fig. 4 as well for the LD1 and LD2, respectively. They are obviously in a linear relation with the ratio $\kappa_{\text{ssym/sym}} = 1.85 \pm 0.06$. In a comparative study on the extraction of $a_{\text{sym}}(A)$ [36], there is a crossover point at $A = 260$ via various mass formulas or local mass relations. The corresponding symmetry energy coefficient is $a_{\text{sym}}(260) = 22.90 \pm 0.15$ MeV, which is very close to the present value in the LD2 extraction, namely, $a_{\text{sym}}(260) = 22.74 \pm 0.16$ MeV. Encouraged by these, it is hoped that the present volume and surface symmetry energy coefficients plus their ratio can be valuable when constraining the symmetry energy coefficient in the nuclear EOS [50,51].

IV. SUMMARY

To summarize, two popular types of liquid drop mass formulas are employed here to make systematical analysis on the model uncertainty via the nonparametric bootstrap strategy. Through repetitive samplings, the least required proportion of the total experimental binding energies in the fitting of mass formula is carefully investigated to not only reducing the computation cost, but also overcome the overfitting problem to some extent. Within this fixed ratio (about 30% of the total data) in the resamplings, the uncertainties of model parameters are then obtained by the present statistical method, leading to the evaluation on the extrapolation ability of the LD formula. This is exemplified by the uranium isotopic chain in which the model uncertainty is found to be generally comparable to the original standard deviation towards the dripline of nuclear chart. In other words, the LD mass formula can provide a relatively robust extrapolation above the systematic error in view of the model uncertainty itself. Owing to the large number of samplings, the correlation analysis is easily performed for the coefficient of each term in the mass formula. Besides the expected situation, the correlation between the coefficients of the symmetry and Wigner energies is placed special attention, reconfirming the necessity of the introduction of the Wigner term especially in the reasonable extraction of the symmetry energy coefficient. Within the present $a_{\text{sym}} = (a_{\text{sym}} + a_{\text{ssym}}/A^{1/3})$, the optimal $a_{\text{sym}} = 32.04 \pm 0.59$ and $a_{\text{ssym}} = -59.35 \pm 3.09$ MeV is suggested plus their ratio $\kappa_{\text{ssym/sym}} = 1.85 \pm 0.06$, which is expected to be useful for constraining the symmetry energy of nuclear equation of state.

[1] D. Lunney, J. M. Pearson, and C. Thibault, Rev. Mod. Phys. **75**, 1021 (2003).

[2] A. C. Larsen, A. Spyrou, S. N. Liddick, and M. Guttormsen, Prog. Part. Nucl. Phys. **107**, 69 (2019).

[3] T. Yamaguchi, H. Koura, Y. A. Litvinov, and M. Wang, Prog. Part. Nucl. Phys. **120**, 103882 (2021).

[4] P. Möller, A. J. Sierk, R. Bengtsson, H. Sagawa, and T. Ichikawa, Phys. Rev. Lett. **103**, 212501 (2009).

[5] P. Möller, A. J. Sierk, T. Ichikawa, and H. Sagawa, At. Data Nucl. Data Tables **109-110**, 1 (2016).

[6] M. Liu, N. Wang, Y. Deng, and X. Wu, Phys. Rev. C **84**, 014333 (2011).

[7] N. Wang, M. Liu, X. Wu, and J. Meng, Phys. Lett. B **734**, 215 (2014).

[8] S. Goriely, S. Hilaire, M. Girod, and S. Péru, Phys. Rev. Lett. **102**, 242501 (2009).

[9] S. Goriely, N. Chamel, and J. M. Pearson, Phys. Rev. C **82**, 035804 (2010).

[10] J. Duflo and A. P. Zuker, Phys. Rev. C **52**, R23(R) (1995).

[11] L. Neufcourt, Y. Cao, S. A. Giuliani, W. Nazarewicz, E. Olsen, and O. B. Tarasov, Phys. Rev. C **101**, 044307 (2020).

[12] M. Kortelainen, J. McDonnell, W. Nazarewicz, E. Olsen, P.-G. Reinhard, J. Sarich, N. Schunck, S. M. Wild, D. Davesne, J. Erler, and A. Pastore, Phys. Rev. C **89**, 054314 (2014).

[13] J. Barea, A. Frank, J. G. Hirsch, P. Van Isacker, S. Pittel, and V. Velázquez, Phys. Rev. C **77**, 041304(R) (2008).

[14] M. Bao, Z. He, Y. Lu, Y. M. Zhao, and A. Arima, Phys. Rev. C **88**, 064325 (2013).

[15] G. J. Fu, Y. Lei, H. Jiang, Y. M. Zhao, B. Sun, and A. Arima, Phys. Rev. C **84**, 034311 (2011).

[16] M. Centelles, X. Roca-Maza, X. Vinas, and M. Warda, Phys. Rev. Lett. **102**, 122502 (2009).

[17] M. W. Kirson, Nucl. Phys. A **798**, 29 (2008).

[18] T. Dong and Z. Ren, Phys. Rev. C **82**, 034320 (2010).

[19] J. Toivanen, J. Dobaczewski, M. Kortelainen, and K. Mizuyama, Phys. Rev. C **78**, 034306 (2008).

[20] C. Yuan, Phys. Rev. C **93**, 034310 (2016).

[21] B. Cauchois, H. Lü, D. Boilley, and G. Royer, Phys. Rev. C **98**, 024305 (2018).

[22] N. Wang and M. Liu, Phys. Rev. C **84**, 051303(R) (2011).

[23] J. S. Zheng, N. Y. Wang, Z. Y. Wang, Z. M. Niu, Y. F. Niu, and B. Sun, Phys. Rev. C **90**, 014303 (2014).

[24] Z. Niu and H. Liang, Phys. Lett. B **778**, 48 (2018).

[25] R. Utama, J. Piekarewicz, and H. B. Prosper, Phys. Rev. C **93**, 014311 (2016).

[26] R. Utama and J. Piekarewicz, Phys. Rev. C **96**, 044308 (2017).

[27] X. H. Wu and P. W. Zhao, Phys. Rev. C **101**, 051301(R) (2020).

[28] B. Efron, *The Jackknife, the Bootstrap and Other Resampling Plans* (SIAM, Philadelphia, 1982).

[29] B. LeBaron and A. S. Weigend, IEEE Trans. Neural Networks **9**, 213 (1998).

[30] E. Zio, IEEE Trans. Nucl. Sci. **53**, 1460 (2006).

[31] R. N. Pérez, J. Amaro, and E. R. Arriola, Phys. Lett. B **738**, 155 (2014).

[32] B. Cai, G. Chen, J. Xu, C. Yuan, C. Qi, and Y. Yao, Phys. Rev. C **101**, 054304 (2020).

[33] J. Jia, Y. Qian, and Z. Ren, Phys. Rev. C **104**, L031301 (2021).

[34] H. A. Bethe and R. F. Bacher, Rev. Mod. Phys. **8**, 82 (1936).

[35] P. Danielewicz, Nucl. Phys. A **727**, 233 (2003).

[36] N. Wang, M. Liu, H. Jiang, J. L. Tian, and Y. M. Zhao, Phys. Rev. C **91**, 044308 (2015).

[37] R. F. Casten, *Nuclear Structure from a Simple Perspective* (Oxford University Press, Oxford, 2000), Vol. 23.

[38] M. Wang, G. Audi, F. G. Kondev, W. Huang, S. Naimi, and X. Xu, Chin. Phys. C **41**, 030003 (2017).

[39] M. Baldo and G. Burgio, Prog. Part. Nucl. Phys. **91**, 203 (2016).

[40] Y. Y. Cheng, M. Bao, Y. M. Zhao, and A. Arima, Phys. Rev. C **91**, 024313 (2015).

[41] J. Dong, W. Zuo, J. Gu, and U. Lombardo, Phys. Rev. C **85**, 034308 (2012).

[42] J. Pu, Z. Zhang, and L.-W. Chen, Phys. Rev. C **96**, 054311 (2017).

[43] L.-W. Chen, C. M. Ko, and B.-A. Li, Phys. Rev. Lett. **94**, 032701 (2005).

[44] M. B. Tsang, Y. Zhang, P. Danielewicz, M. Famiano, Z. Li, W. G. Lynch, and A. W. Steiner, Phys. Rev. Lett. **102**, 122701 (2009).

[45] I. Talmi, *Simple Models of Complex Nuclei The Shell Model and Interacting Boson Model* (Harwood Academic, Switzerland, 1993).

[46] E. Wigner, Phys. Rev. **51**, 106 (1937).

[47] E. Wigner, Phys. Rev. **51**, 947 (1937).

[48] M. W. Kirson, Phys. Lett. B **661**, 246 (2008).

[49] G. Royer and C. Gautier, Phys. Rev. C **73**, 067302 (2006).

[50] H. Jiang, G. J. Fu, Y. M. Zhao, and A. Arima, Phys. Rev. C **85**, 024301 (2012).

[51] B. K. Agrawal, J. N. De, and S. K. Samaddar, Phys. Rev. Lett. **109**, 262501 (2012).